Available online at www.sciencedirect.com
SCIENCE DIRECT
Surface & Coatings Technology 199 (2005) 57 – 65
SURFACE & COATINGS TECHNOLOGY
www.elsevier.com/locate/surfcoat

Adhesion behaviour of CrN_x coatings on pre-treated metal substrates studied in situ by PBA and ESEM after annealing

R. Escobar Galindo[a,*], A. van Veen[a], H. Schut[a], G.C.A.M. Janssen[b], R. Hoy[b], J.Th.M. de Hosson[c]

[a]*Interfaculty Reactor Institute, Delft University of Technology, Mekelweg 15, NL-2629 JB Delft, The Netherlands*
[b]*Department of Materials Science and Technology, Delft University of Technology, Rotterdamseweg 137, NL-2628 AL, The Netherlands*
[c]*Materials Science Centre and NIMR, University of Groningen, Nijenborgh 4, NL-9747 AG Groningen, The Netherlands*

Received 14 April 2004; accepted in revised form 11 April 2005
Available online 24 May 2005

Abstract

In this paper we present the first combined Positron Beam Analysis (PBA) and Environmental Scanning Electron Microscopy (ESEM) adhesion study on thin chromium nitride (CrN_x) coatings. Both techniques are combined with a 4-point bending stage. PBA monitors the creation of open volume in the ceramic/metal interface prior to delamination while ESEM observations provide a picture of the delamination process itself. By varying the positron implantation energy, the coating layer or the coating/substrate interface can be studied separately. Coatings of 500 nm thickness were deposited via a physical vapour deposition (PVD) process on different types of steel and on polycrystalline copper. Samples were studied as deposited, after 30 min annealing at 973K, and during the 4-point bending test, respectively. After annealing the PBA results have changed depending on the substrate and the treatment. The positron *S* parameter associated to the nitride coating increases over the whole layer for samples deposited on tool steel and polycrystalline copper. In the case of the CrN_x layers deposited on interstitial free steel, there is a lower *S* parameter in the first 75 nm of the coating. This 2-layer structure inside the coating is more pronounced if the substrate is implanted with metal ions prior to the deposition. The positron parameter changes observed in the coatings after annealing are confirmed by ESEM observations and it is related to the structural changes in the coating. The *S* value ascribed to the interface increases in all samples after the annealing process confirming the creation of open volume at the interface. The 4-point bending tests revealed a plastic deformation of the coating deposited on the soft IF substrate and a brittle delamination of the film when deposited on the hard tool steel.

Keywords: Adhesion behaviour; CrN_x coatings; Pre-treated metal substrates; Positron Beam Analysis (PBA); Scanning electron microscopy

1. Introduction

Chromium nitride (CrN_x) films deposited by Physical Vapour Deposited (PVD) have been used extensively in the industry due to their excellent mechanical properties [1–7], corrosion resistance [8,9] and excellent wear behaviour [10–13]. Applications of CrN_x coatings are found in cutlery, aeronautical and textile industry as well as in the technology for protection of cutting tools and dies. In recent years CrN_x films have also been used to replace hard chromium for specific applications in the automotive industry [14,15]. Among the advantages of CrN_x coatings are the reduced coefficient of friction, the lower internal stresses and the possibility of using thick coatings. For example CrN_x coatings with a thickness of 40 μm are routinely used by one of the largest Japanese piston ring supplier [15].

As these films are normally used at high temperatures, the influence of heat treatments on the mechanical, tribological and corrosion properties of the coatings is of great interest. Changes of the coating adhesion and the wear

* Corresponding author. Departamento de Física e Ingeniería de Superficies, Instituto de Ciencia de Materiales de Madrid, Consejo Superior de Investigaciones Científicas, Cantoblanco, 28049 Madrid, Spain. Tel.: +34 91 3721420; fax: +34 91 3720623.
E-mail address: rescobar@icmm.csic.es (R. Escobar Galindo).

0257-8972/$ - see front matter © 2005 Elsevier B.V. All rights reserved.
doi:10.1016/j.surfcoat.2005.04.018

resistance of different PVD coatings after vacuum annealing have been reported in [16], while the oxidation of the CrN_x coatings has been studied in [17] as a function of the annealing atmosphere.

In this work we used Positron Beam Analysis (PBA) together with Environmental Scanning Electron Microscopy (ESEM) to study the behaviour of very thin CrN_x films during annealing and bending experiments. In fact, this paper is intended to be a demonstration of the potential PBA capabilities for investigating interfacial properties of hard coatings in combination with other more standard material research techniques (i.e. scanning electron microscopy). PBA is a non-destructive technique suitable for the study of open volume due to the preferential trapping of positrons in defects or low-density regions [18]. By varying the positron implantation energy, the coating layer or the coating/substrate interface can be monitored separately. Due to its non-destructive nature, PBA allows in situ characterization of changes occurring at the interfaces or the bulk of the samples during annealing or bending experiments.

In a previous article [19] we showed the first PBA results obtained during in situ bending experiments on CrN_x, TiN and Diamond Like Carbon (DLC) thin films with thicknesses larger than 1.5 μm. In the present paper we focus on thinner CrN_x layers (500 nm) in order to have a better insight of the interface characterization by PBA.

2. Experimental

500 nm CrN_x coatings were deposited on different metal substrates (1 mm thick) using an industrial Hauzer HC 750 PVD sputtering machine. A special feature of this machine is that not only a plasma in front of the target is present, but also that all of the chamber can be filled with a plasma created by a bucket source placed on top of the deposition chamber [20]. A chromium target (122 × 600 mm) was used for deposition. The flow of argon gas was 115 sccm and the nitrogen gas flow was 45 sccm. The substrates performed a planetary motion in front of the target. Minimum target to substrate distance was 25 cm. A negative bias voltage of − 225 V was applied to the substrates during the deposition. The bias current was 2.5 A, thus, with an estimated carrousel area of 0.3 m^2, this means a substrate current density of 8.3 A/m^2 or an ion to atom arrival rate of 2.3. The power applied to the target was 5 kW, leading to a target voltage of 500 V and a target current of 10 A. The working pressure in the deposition chamber was typically of 0.4 Pa. The films were deposited at 450 °C (with the temperature remaining constant during deposition process) with a deposition time of 35 min and a composition CrN_x ($x = 0.45$). More details about the deposition procedure are explained in [20,21].

Prior to the deposition of the coating, the metal substrates were mechanically polished down to 1 μm roughness with a mirror-like appearance after a silica solution finishing. Subsequently, to provide a defect-free surface, the substrates were annealed in a vacuum of typically 10^{-5} Pa. The steel substrates were annealed for 1 h at 1000 K while the polycrystalline copper substrates were annealed for 30 min at 873 K in the presence of hydrogen (5×10^{-5} Pa) to avoid copper oxidation. Finally the substrates were ultrasonically cleaned, first with acetone and finally with ethyl alcohol. This substrate pre-treatment is the "normal" treatment mentioned in Table 1 where an overview of the deposited samples is given. Additionally to this treatment and in order to provide a modified surface to the coating deposition, one of the tool steel (TS3) and one of the Interstitial Free steel (IF4) substrates were implanted with Zn ions at 34 keV with a fluency of 10^{16} ions cm^{-2} while another tool steel (TS4) substrate was oxidized during the annealing procedure after polishing. A similar implantation treatment with helium has been found to produce a dramatically surface modification in metals upon annealing [22]. Coatings deposited on different pre-treated substrates are expected to show differences at the interfaces. The differences observed at the various coating/substrate interfaces will be one of the main topics of discussion in our work.

The samples were studied by Positron Beam Analysis and Environmental Scanning Electron Microscope (ESEM) after the coating deposition ("As received" in Table 1), after a post-deposition annealing of 30 min in a vacuum of

Table 1
Description of the thin 500 nm CrN_x coatings studied showing the different substrate pre-treatment and the experimental techniques applied to each sample

Substrate	Code	Pre-treatment	As received		Post-annealing		Bending	
			VEP	ESEM	VEP	ESEM	VEP	ESEM
Tool steel	TS1	Normal	+	+				+
	TS2	Normal					+	
	TS3	Zn implanted	+	+	+	+		+
	TS4	Oxidized	+	+			+	
IF steel	IF1	Normal	+	+				+
	IF2	Normal					+	
	IF3	Zn implanted	+	+	+	+		
	IF4	Normal			+	+		
Stainless steel	SS1	Normal	+	+				+
Copper	CU1	Normal	+	+				
	CU2	Normal			+	+		

typically 10−5 Pa at 973 K ("Post-Annealing" in Table 1) and during 4-point bending ("Bending" in Table 1) inside the ESEM and the positron beam line, respectively. A short description of each analysis techniques is given below.

Positron Beam Analysis (PBA) was performed using the Delft Variable Energy Positron beam (VEP) [23]. The positrons are injected into the samples with energies tuned between 100 eV and 25 keV. The maximum implantation energy corresponds to a typical mean implantation depth of ~2 μm in materials with density ~3 g cm^{-3}. All experiments were carried out at room temperature under a vacuum of about 10^{-6} Pa. PBA results are described in terms of two parameters. The S parameter [24] indicates the fraction of positrons that annihilates with low momentum electrons (valence or conduction electrons). This parameter is related to the open volume defects present in the sample (e.g. vacancy clusters, interfaces with misfit). In general, a high value of S indicates positron annihilation in open volume defects. The W parameter [25] indicates the fraction of positrons that annihilates with high momentum electrons (core electrons). This parameter is related to the chemical environment where the annihilation takes place. Both parameters can be combined in $S-W$ maps with a third variable (e.g., the implantation depth, the sample temperature or strain) as a running parameter. These maps are useful to trace positron trapping in, e.g., layers as a function of temperature as in the samples described in this work. The data were analysed with the Variable Energy Positron Fit (VEPFIT) program [26]. This program describes the sample by a number of stacked layers. Each of these layers is characterized by its thickness (D_i), the S_i and W_i parameters and the positron diffusion length (L_i). Although positron annihilation sites can be distinguished at the surface, bulk of the coating, coating–substrate interface and the substrate, the coating and the interface values are the most interesting ones for this study.

A Philips XL30 Environmental Scanning Electron Microscope (ESEM) of the Materials Science Department of the University of Groningen was used to observe the coatings in situ during bending experiments. Both the positron Beam and the ESEM are equipped with a bending module from Kammrath and Weiss GmbH. This module allows performing 4-point bending experiments, both in compressive and tensile mode. The samples subjected to bending tests were notched in order to enhance delamination in the specimen [27,28]. The notches were performed, using a diamond saw, on the backside of the substrates with a depth of approximately half of the substrate thickness.

3. Results and discussion

3.1. PBA on as deposited thin CrN_x coatings

In Fig. 1(a) the PBA experimental results on the as deposited samples on tool steel (TS1) and IF steel (IF1) with

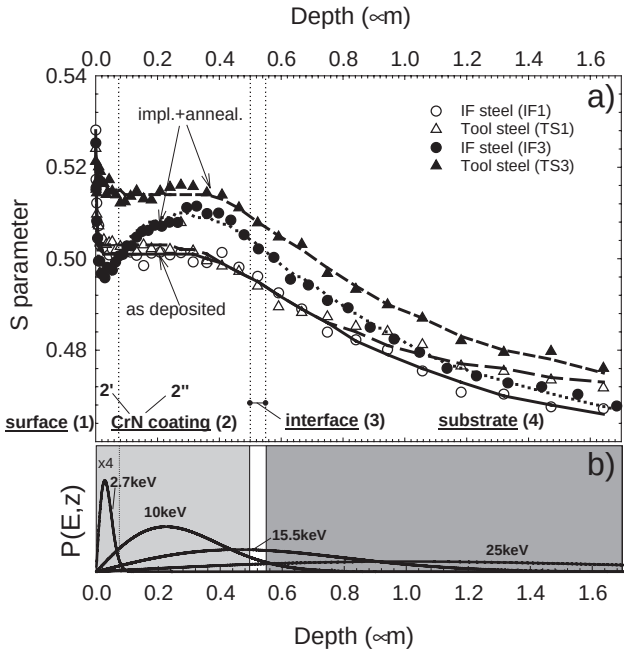

Fig. 1. Doppler Broadening results on the thin CrN_x films. In (a) the S parameter is plotted as a function of the positron mean implantation depth for samples as deposited and after annealing on IF and tool steel. The lines represent the VEPFIT analysis results. The coating deposited on IF the CrN_x layer splits in two (2′ and 2″) after annealing. In (b) are shown the positron implantation profiles $P(E,z)$ in the middle of the different layers. The labels indicate the corresponding implantation energies.

"normal" pre-treatment are presented (white symbols). The S parameter is plotted versus the positron mean implantation depth. The mean implantation depth was obtained from the positron implantation energy using a density of 5.9 g cm^{-3} in the whole sample. The samples are described in terms of four layers, each of them associated to different positron annihilation sites: (1) surface, (2) 500 nm CrN_x coating, (3) 10-nm coating–substrate interface, and (4) metal substrate as can be seen in the scheme of Fig. 1(b). Superimposed to that scheme typical positron implantation profiles are plotted for different implantation energies corresponding to implantation in the coating (2.7 and 10 keV), the interface (15.5 keV) and the substrate (25 keV). It can be clearly observed how the implantation profiles become broader with the increase of positron energy. This straggling results at the higher energies in significant contributions from more than one layer. For example at implantation energy of 15.5 keV, related to implantation at the interface, there are also significant fractions of positrons implanted at the coating and the substrate. This is the reason why the S-curves of Fig. 1(a) show a gradual change from the coating to the substrate without a clear indication of the interface.

In order to enhance the positron signal from the interface both the S and W parameters are combined in a $S-W$ map as the ones shown in Fig. 2(a and (b). In such maps it can be seen that the experimental data of the as deposited samples (black symbols) do not follow a straight line from the

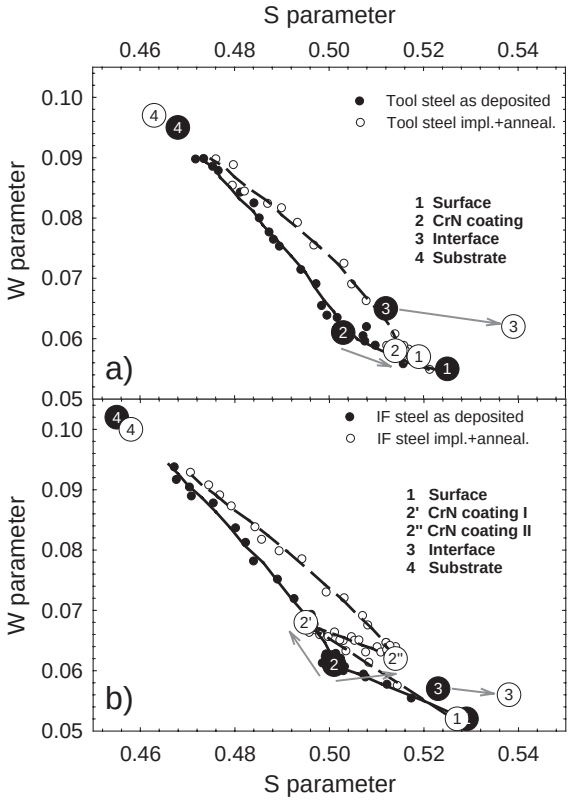

Fig. 2. Doppler Broadening results on the thin CrN_x films. The $S-W$ maps for samples as deposited and after annealing on (a) tool steel and (b) IF are shown, respectively. The solid lines represent the VEPFIT analysis results. The numbered circles indicate the positron annihilation sites ascribed to (1) Surface, (2) Coating layer, (3) Interface, and (4) Substrate. The arrows indicate the changes observed in the coating and the interface after annealing treatment.

coating (2) to the substrate (4). This change in the linear behaviour of S and W is related to the positron annihilation at the interface (3). The lines drawn in Fig. 1(a) and Fig. 2 are the fitting result using the VEPFIT program. This program takes into account the above-mentioned implantation profiles and associates S and W values (cluster points) to the different layers of the system. These cluster points are plotted in Fig. 2 using large numbered circles.

The results of VEPFIT analysis are summarised in Table 2. In Fig. 3 the fitted S parameters are plotted as a function of depth for all the samples. It can be observed that for all the substrates the as deposited CrN_x layer (2) is homogeneous as the S and W parameters are constant through the coating thickness. A different interface (3) is observed for the sample TS4 as compared to TS1. This is due to the oxide layer (approximately 100 nm thick) present before deposition. For comparison purposes a non-coated but pre-oxidized tool steel sample was also studied. The S and W parameters ascribed to the oxide were found to be ($S=0.539$, $W=0.057$). In Table 2 can be observed that after implantation there are no changes either in the coating or in the substrate. This indicates that the deposited ions did not migrate towards the interfaces at the deposition temperatures and that the damage created on the substrate during implantation was below the detection limit of the PA technique.

3.2. PBA–ESEM study on annealed thin CrN_x films

After annealing the PBA results are different depending on the type of substrate as can be observed in Figs. 1(a) and 2 (black symbols) for the coatings deposited on tool and IF steel. As in the case of as deposited samples the lines are the fitting result from VEPFIT. The results of the VEPFIT analysis are also presented in Table 2. In the samples deposited on tool steel after the implantation and annealing process, an increase of S over the whole layer thickness is observed (see Fig. 1(a)). This change is also observed in the position of the cluster point (2) in the $S-W$ map of Fig. 2(a). On the other hand, when the coating is deposited on IF steel there is first a decrease of the S parameter followed by subsequent increase of S on increasing coating thickness (see Fig. 1(a)). In the $S-W$ map of Fig. 2(a) this effect is monitored by the appearance of two cluster points (2′ and 2″) characterizing the CrN_x coating. This is observed both

Table 2
VEPFIT results on the different 500 nm CrN_x samples studied: S and W parameters inside the coating (at depths of 75 and 500 nm) and at the interface, and the positron diffusion length l_{coat} inside the coatings

Sample	S_{coat}, 75 nm	W_{coat}, 75 nm	l_{coat} (nm), 75 nm	S_{coat}, 500 nm	W_{coat}, 500 nm	l_{coat} (nm), 500 nm	S_{interf}	W_{interf}
TS1	0.503	0.061	1.5	0.503	0.061	1.5	0.512	0.065
TS3	0.503	0.061	2.8	0.503	0.061	2.8	0.513	0.066
TS3 ann.	0.514	0.058	10	0.514	0.058	10	0.539	0.062
TS4	0.503	0.062	3.3	0.503	0.062	3.3	0.539	0.057
IF1	0.501	0.061	1.5	0.501	0.061	1.5	0.523	0.057
IF3	0.501	0.061	1.5	0.501	0.061	1.5	0.518	0.059
IF3 ann.	0.495	0.068	4.7	0.511	0.065	11.8	0.531	0.052
IF4 ann.	0.497	0.067	10	0.512	0.065	1.5	0.538	0.056
SS1	0.503	0.062	3	0.503	0.062	3	0.500	0.065
CU1	0.502	0.061	2	0.502	0.061	2	0.530	0.073
CU2 ann.	0.510	0.059	8	0.510	0.059	8	0.534	0.078

The typical error in S and W parameter affects the last decimal.

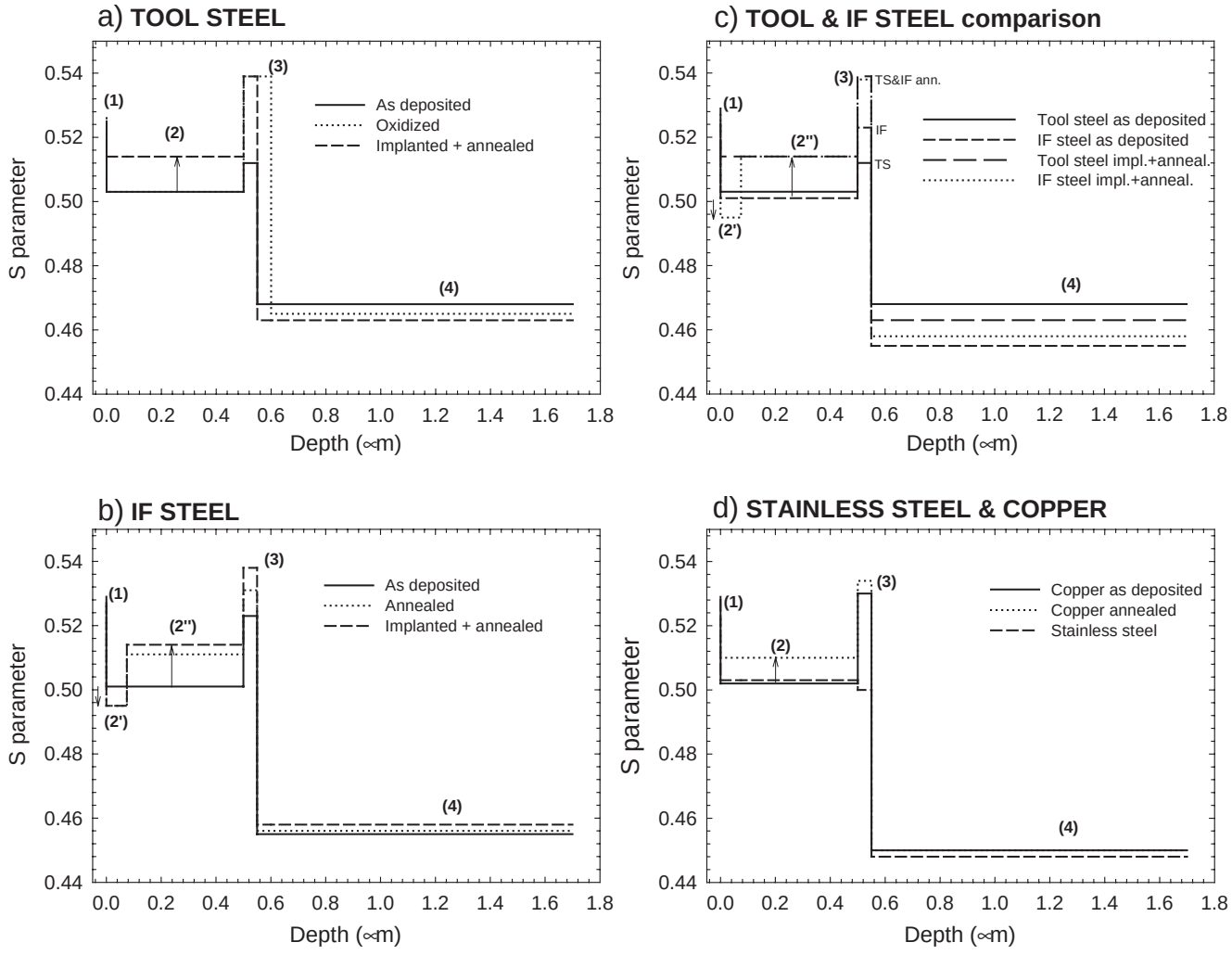

Fig. 3. Doppler Broadening results on the thin CrN_x films. The S parameter obtained from VEPFIT is plotted versus the positron mean implantation depth for the different coatings deposited on (a) tool steel, (b) IF steel and (d) stainless steel and copper substrates. In (c) there is a comparison between the results obtained on IF and tool steel before and after implantation with annealing treatment.

for the implanted (IF3) and non-implanted (IF4) samples (see Table 2) and indicates a layered structure of the coatings. The thickness of the first layer (2′) is estimated from VEPFIT to be 75 nm, while the second (2″) is 425 nm thick. The $S-W$ cluster point associated to the interface (3) moves in both cases towards higher (lower) values of S (W) (see Fig. 2). The changes in S after the different treatments are clearly seen as a function of depth for all the samples in Fig. 3.

In Fig. 3(b) it can be observed that the layered structure is also present for samples deposited on IF steel after annealing without pre-implantation (sample IF4). The S value of the second layer inside the coating (2″) and the interface (3) for the annealed sample are lower than the ones for the implanted and annealed samples. In Fig. 3(c) a comparison between the previously described effects of implantation and annealing on coatings deposited on tool and IF steel is made. It is interesting to note that the S value of (2″) and (3) are the same for the implanted and annealed samples. Finally, it can observed in Fig. 3(d) that the annealed coating deposited on polycrystalline copper also shows an increase of the S parameter over the whole layer thickness as in the case of the samples deposited on tool steel but with a lower S.

In Fig. 4 a summary of the S values obtained from VEPFIT in (a) the first 75 nm (2′) and (b) from 75 to 500 nm (2″) inside the coating and (c) at the coating metal interface (3) are plotted for all the different samples and treatments. As mentioned before, the S parameter ascribed to the whole nitride coating (2) increases for both samples deposited on the implanted tool steel (TS3) and the non-implanted polycrystalline copper (CU2) after annealing. This increase in S is related to an increase of the open volume in the layers. In the case of the IF steel the S parameter inside the coating is lower compared to the as deposited samples in the first 75 nm (2′) indicating a densification of the layer. Then

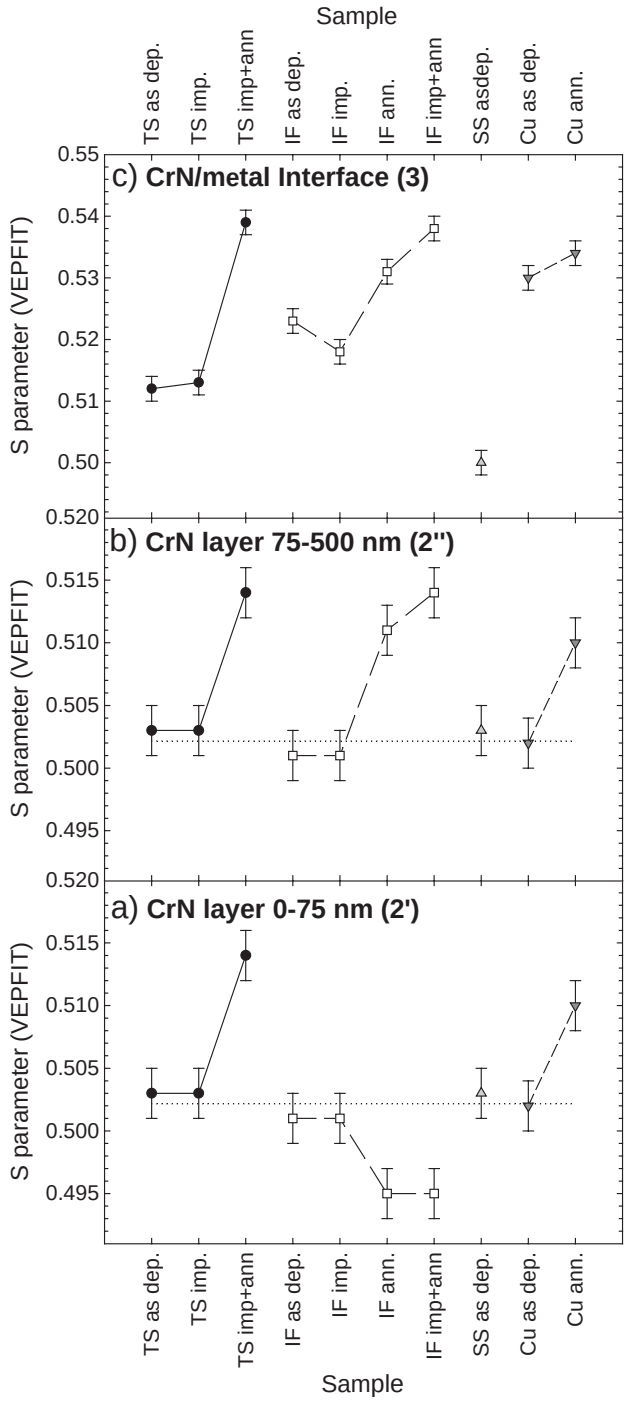

Fig. 4. *S* values obtained from VEPFIT are plotted for the different samples (a) at 75 and (b) at 500 nm deep inside the coating and (c) at the coating metal interface.

it increases towards an *S* value similar to the TS3 and CU2 annealed samples. This behaviour seems to be more pronounced on the implanted sample IF3 (higher *S* and lower positron diffusion length in the second layer). This different behaviour of the coating after annealing depending on the substrate is related to its adhesion properties. As can be seen in Fig. 4 the *S* value ascribed to the interface (3) increases in all samples after the annealing process. This is related to the creation of open volume at the interface and therefore to the first stages of delamination of the coating from the substrate.

ESEM side views of samples TS3, TS4, IF1 and IF3 are shown in Fig. 5. For the implanted and annealed samples it is observed how the IF3 (Fig. 5(c)) presented a double layer structure while for the TS3 sample (Fig. 5(d)) the 500-nm layer is preserved. This fits very nicely with the PBA experiments as can be observed in the superimposed *S* versus depth graphs of Fig. 5. The mean implantation depth was obtained from the positron implantation energy assuming a density of 5.9 g cm^{-3} in the sample. There is certain discrepancy in the thickness of the layers in sample IF3. According to ESEM observations the first layer has a thickness of ~200 nm and the second layer is ~700 nm thick while VEPFIT analysis results in thinner layers of 75 and 425 nm, respectively.

3.3. *In situ* bending thin CrN_x coatings

Four-point bending experiments in compression were performed in situ the positron beam on notched samples IF1, TS1 and SS1. The positron experiments were carried out at implantation depths of 100 eV and 5, 10, 15, 20 and 25 keV. These implantation energies correspond approximately to a mean implantation depth at the surface of the layer, 95, 290, 550, 880 and 1255 nm, respectively, again assuming a density of 5.9 g cm^{-3}. Note that for the last two implantation energies there is a large contribution from the steel substrate ($\rho = 7.9$ g cm^{-3}) and therefore the mean implantation depth is shorter (but always larger than the coating thickness). This has no influence in the following discussion.

No significant changes were observed in the *S* parameter after bending experiments for implantation energies lower than 15 keV. This indicates that from the positron point of view neither the surface nor the bulk of the coatings has changed during bending. Although the changes are small there is a trend of increasing *S* parameter with the bending displacement. This increase of *S* is related to the appearance of first defects prior to the delamination of the coatings for experiments performed at 15 and 20 keV. On the other hand the increase of *S* during bending at the highest implantation depth (25 keV) is related to the creation of small defects (vacancies) in the metal substrate.

Similar bending experiments were performed inside the ESEM on notched samples TS2, TS4 and IF2. A selection of pictures obtained is presented in Figs. 6, 7 and 8, before and after bending. Different delamination processes can be observed depending on the type of substrate.

In Fig. 6 the brittle delamination of the coating deposited on hard tool steel is seen. Parts of the coating are removed during the bending process. This type of delamination is enhanced in the presence of an oxide layer as can be observed in Fig. 7 for the coating deposited on oxidized tool

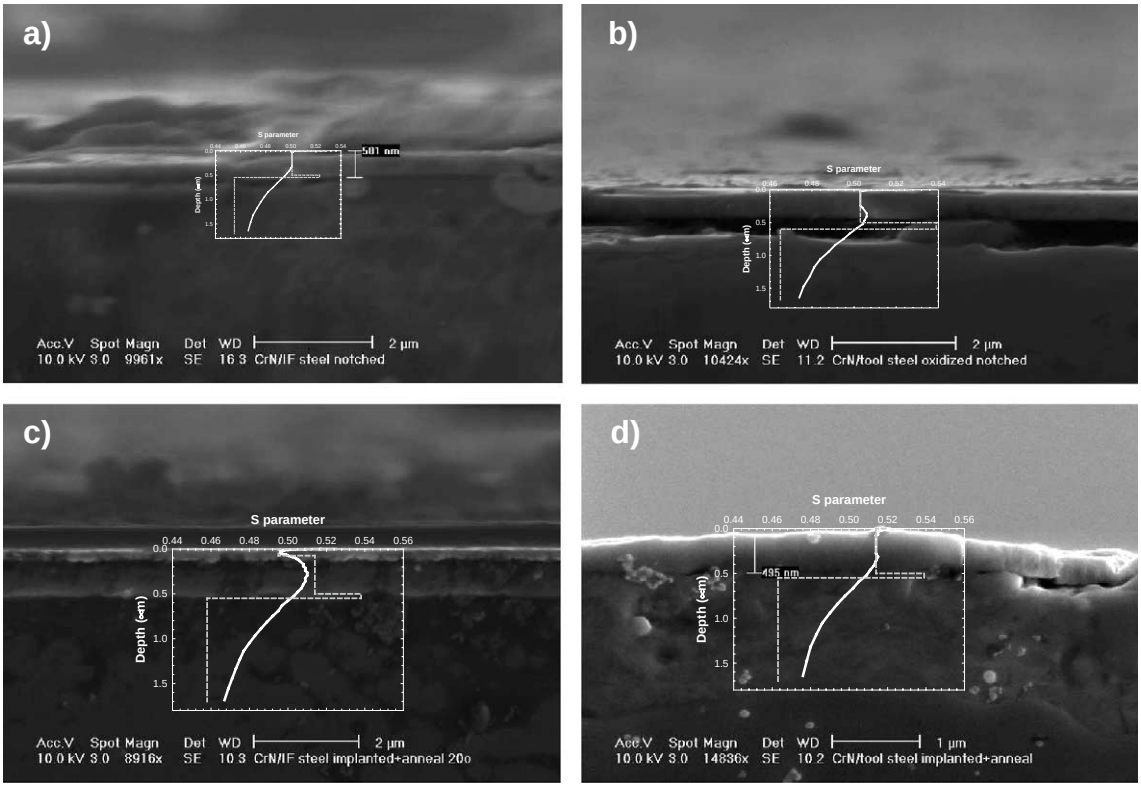

Fig. 5. ESEM side views micrographs are shown of CrN_x samples (a) as deposited on IF steel (IF1), (b) as deposited on pre-oxidized tool steel (TS4), (c) after annealed on implanted IF steel (IF3) and (d) after annealing on implanted tool steel (TS2). On each micrograph the *S* parameter obtained by VEPFIT is plotted versus the mean positron implantation depth.

steel. The flaking of the coatings is massive even for lower displacements indicating the poor adhesion of the coating to the oxide.

In Fig. 8 the plastic deformation of the soft IF substrate is observed. The coating follows the substrate deformation without delaminating. These effects were not detected by

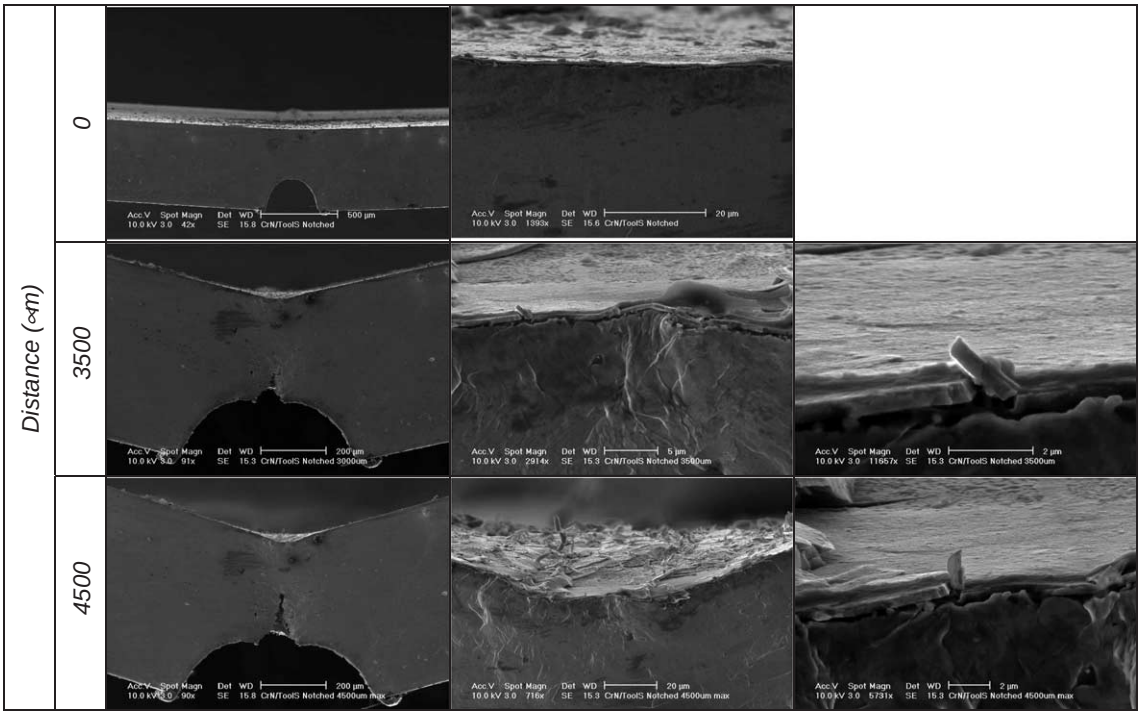

Fig. 6. ESEM pictures of CrN_x deposited on tool steel sample (TS2) before (0 μm), during (3500 μm) and after (4500 μm) in situ bending experiments.

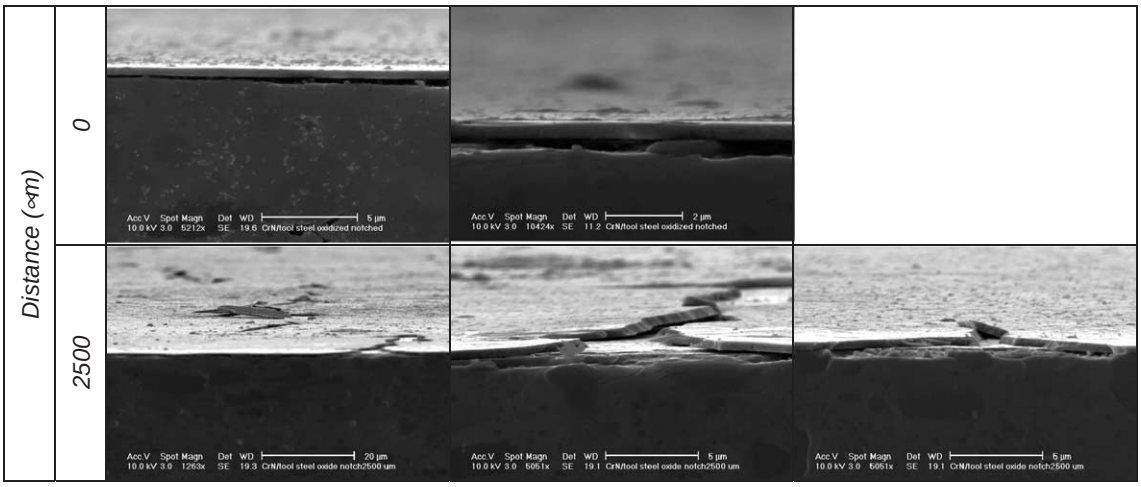

Fig. 7. ESEM pictures of CrN_x deposited on oxidized tool steel sample (TS4) before (0 μm) and after (2500 μm) in situ bending experiments.

PBA because the area where they occur is too small compared to the spot size of the positron beam (8 mm).

4. Conclusions

The combination of Positron Beam Analysis and Scanning Electron Microscopy is a very useful tool to study the bulk and interfacial behaviour of thin ceramic coatings after high temperature annealing and during in situ bending test. Depending on the nature of the substrate a different behaviour was observed for thin CrN_x coatings after annealing at 973 K. Coatings deposited on IF steel presented a double layer structure consisting of a thin dense layer of 75 nm and a thicker layer of 425 nm with a more open structure. For samples deposited on tool steel and polycrystalline copper there is a decrease of the density all over the layers. In all cases there is an open volume increase at the interface related to first stages of coating delamination. In situ bending experiments in the ESEM revealed a brittle delamination of the coatings deposited on tool steel, enhanced by the presence of an oxide layer. The films deposited on IF steel followed the plastic deformation of the soft substrate. Positron experiments during bending,

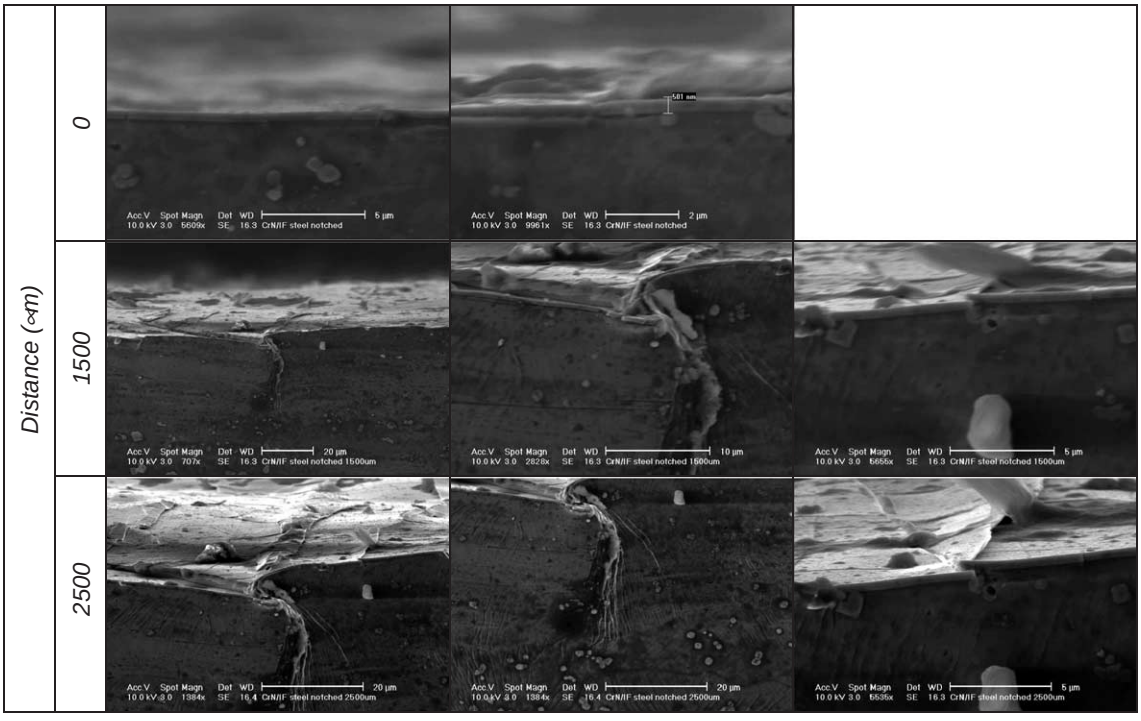

Fig. 8. ESEM pictures of CrN_x deposited on IF steel sample (IF1) before (0 μm), during (1500 μm) and after (2500 μm) in situ bending experiments.

although insensitive to these massive effects, detected the formation of defects prior to the delamination of the coatings.

Summarizing, PBA monitors, in a non-destructive manner, the creation of open volume in the coating/metal interface prior to delamination and structural changes of the coating upon annealing. These PBA "observations" were nicely correlated to ESEM real observations providing a clear picture of the first stages of the delamination of the coating. In our opinion, this work emphasises the potential use of PBA in combination with standard material research characterization techniques to elucidate characteristics regarding the interface and porosity of thin films.

Acknowledgements

It is with deep sorrow that we have to report the sudden death of Prof. A. van Veen during the preparation of this manuscript. This work was financially supported by the Dutch Technology Foundation STW (project number GTF.4901). We wish to thank M.A. van Huis (Interfaculty Reactor Institute, TUDelft) for the ion implantation of the samples.

References

[1] T. Hurkmans, D.B. Lewis, J.S. Brooks, W.D. Munz, Surf. Coat. Technol. 86–87 (1996) 192.
[2] S.H. Yao, Y.L. Su, Wear 212 (1997) 85.
[3] T. Hurkmans, D.B. Lewis, H. Paritong, J.S. Brooks, W.D. Munz, Surf. Coat. Technol. 114 (1999) 52.
[4] J.N. Tu, J.G. Duh, S.Y. Tsai, Surf. Coat. Technol. 133–134 (2000) 181.
[5] X.M. He, N. Baker, B.A. Kehler, K.C. Walter, M. Nastasi, Y. Nakamura, J. Vac. Sci. Technol., A 18 (2000) 30.
[6] J. Almer, M. Oden, L. Hultman, G. Hakansson, J. Vac. Sci. Technol., A 18 (2000) 121.
[7] H. Janse, U.M. Jansen, G.N. Pederson, G. Sorensen, Surf. Coat. Technol. 59 (1993) 135.
[8] M. Urgen, A.F. Cakir, Surf. Coat. Technol. 96 (1997) 236.
[9] F.D. Lai, J.K. Wu, Surf. Coat. Technol. 64 (1994) 53.
[10] B. Navinsek, P. Panjan, I. Milosev, Surf. Coat. Technol. 97 (1997) 182.
[11] Y.L. Su, J.S. Lin, Wear 170 (1993) 45.
[12] F.D. Lai, J.K. Wu, Surf. Coat. Technol. 88 (1997) 183.
[13] R. Gåhlin, M. Bromark, P. Hedenqvist, S. Hogmark, G. Håkansson, Surf. Coat. Technol. 76–77 (1995) 174.
[14] C. Friedrich, G. Berg, E. Broszeit, F. Rick, J. Holland, Surf. Coat. Technol. 97 (1997) 661.
[15] http://www.hauzertechnocoating.com/pers01.htm.
[16] W. Herr, E. Broszeit, Surf. Coat. Technol. 97 (1997) 669.
[17] F.H. Lu, H.Y. Chen, Thin Solid Films 398 (2001) 368.
[18] A. van Veen, H. Schut, P.E. Mijnarends, in: P. Coleman (Ed.), Positron Beams and their Applications, World Scientific Publishing Co, 2000, (Chapter 6).
[19] R. Escobar Galindo, A. van Veen, N.J. Carvalho, C. Strondl, H. Schut, J.Th.M. de Hosson, Mater. Res. Soc. Proc. 695 (2002) 397.
[20] G.C.A.M. Janssen, R. Hoy, J. Vac. Sci. Technol., A 21 (2003) 569.
[21] R. Hoy, W.G. Sloof, G.C.A.M. Janssen, Surf. Coat. Technol. 179 (2–3) (2004) 215.
[22] R. Escobar Galindo, A. van Veen, J.H. Evans, H. Schut, J.Th.M. de Hosson, Thin Solid Films 471 (2005) 170.
[23] A. van Veen, J. Trace Microprobe Tech. 8 (1990) 1.
[24] I.K. MacKenzie, J.A. Eady, R.R. Gingerich, Phys. Lett. 33 (1970) 279.
[25] P.H. Leo, K.D. Moore, P.L. Jones, F.H. Cocks, Phys. Status Solidi B 108 (1981) K145.
[26] A. van Veen, H. Schut, J. de Vries, R.A. Hakvoort, M.R. IJpma, in: P.J. Schultz, G.R. Massoumi, P.J. Simpson (Eds.), American Institute of Physics 218, Positron Beams for Solids and Surfaces, 1990, p. 171.
[27] N. Barbosa III, R.S. Ridley, C.H. Strate, R.S. Dwyer, T. Grebs, R.P. Vinci, Mater. Res. Soc. Proc. 695 (2002) 341.
[28] H.G.P. Chung, M.V. Swain, T. Mori, Biomaterials 18 (23) (1997) 1553.